P1.13 DEMONSTRATION OF A RELOCATABLE HIGH-RESOLUTION, RAPID-RESPONSE METEOROLOGICAL MODEL SUITABLE FOR FOREST FIRE RESPONSE NOWCASTING

Nelson L. Seaman*, David R. Stauffer, Annette M. Gibbs,
Aijun Deng, Anthony J. Schroeder, and Glenn K. Hunter

The Pennsylvania State University
Department of Meteorology, University Park, PA

1. INTRODUCTION

The semi-arid climate and mountainous scrub-and-forest topography of the American West combine to make this area one of the most vulnerable to forest fires in North America, as well as one of the most difficult in which to combat wild fires. Frequent drought conditions in summertime often cause the fire danger to become extreme. Moreover, the remoteness of many areas make it exceptionally difficult to combat fires. Add to this the uncertainty associated with rapidly changing weather conditions, and situations are created for fire fighters in which almost any blaze can behave unpredictably and suddenly become life threatening. The recent tragic deaths of four fire fighters in the northern Cascade Mts. of Washington on 11 July 2001 provides a sobering example (Jackson 2001).

In such dangerous conditions, access to accurate up-to-the-minute computer-generated *"nowcasts"* of local meteorology (wind, temperature, humidity, lightning storms, etc.) in rugged mountainous areas can be of tremendous value. Unfortunately, most operational numerical weather prediction models are run only twice per day and have grid resolutions that fail to represent accurately much of the complex topography of the western states. Thus, despite their considerable value, they lack the spatial and temporal resolution needed to best protect front-line crews responding to current conditions as they attempt to control dangerous blazes. The *motivation* for this study, therefore, is to propose and explore a new methodology for providing inexpensive short-term numerical meteorological guidance to support fire crews on a time scale of minutes to several hours.

1.1 *Time Scales of Meteorological Influences*

This discussion raises an important point that lies at the heart of the issue of meteorological influences on fire danger, that is, the issue of *scale*. For the present, we can focus our attention by considering three time scales. For the western states, the *climate* determines that the summer months have the highest ratio of evaporation versus precipitation, leading to seasonal drying of the potential fuel base. Additional variability on the scale of weeks to months can lead to dangerous drought conditions. Since long-term droughts tend to be associated with slow-changing synoptic patterns on the scale of 5000-15000 km, areas affected by drought often cover large regions of 1000-3000 km square. So, our first critical time scale is on the *monthly-to-seasonal scales* that set up the background conditions that increase the potential for forest fires over broad regions. Much progress has been made in the past decade on the prediction of seasonal temperature and rainfall anomalies and the National Centers for Atmospheric Prediction (NCEP) issues monthly climate forecasts that can be readily used for long term planning up to a year in advance (Barnston et al. 1999). This type of approach relies on a combination of long-running global models, correlation analysis, historical analogues, and statistical processing of these component predictors.

Next, given overall seasonal conditions conducive to combustion, individual weather systems such as a cold front or an upper-level trough often trigger nearly simultaneous outbreaks of numerous forest fires. In distant regions having more abundant atmospheric water vapor, the passage of these *mesoalpha-scale systems* (~200-2000 km) may induce thunderstorms and heavy rain. However, in the drier inter-mountain regions of western North America, these systems often produce lightning, but little or no rain. Given the combination of abundant tinder-dry fuel and a perfect source of widespread intense "sparks", scores of fires can be ignited in a few minutes. Moreover, strong gusty winds associated with fronts and troughs can cause intensification of existing fires. Replacement of relatively moist pre-frontal air by lower humidities in a post-frontal air mass can heighten the combustibility of plant fuels spread on the forest floor. The time scale associated with passage of these frontal and trough features is on the order of 6-24 h. Importantly, current operational numerical weather prediction models (e.g., the NCEP Eta model, Black 1994) have well-documented skill for periods of 1-3 days in advance and can provide reasonable warnings of the approach and severity of such systems. This assists supervisors in planning strategies to maximize the effectiveness of personnel and equipment committed to battle multiple fires over a region. Typically, these mesoscale models have horizontal resolutions of ~20 km and are run on fixed continental-scale domains. Of course, the

*Corresponding author: Nelson L. Seaman, Penn State Univ., Dept. of Meteorology, University Park, PA, 16802. Ph.: 814-863-1583, Fax: 814-865-3663,
Email: seaman@ems.psu.edu

accuracy of such models is far from perfect. Nevertheless, they have tremendous value for providing advanced meteorological warnings for our second critical time scale, the *daily-to-several-day scales*.

Despite the obvious value of mesoalpha-scale predictive models for fire-response planning, it must be recognized that fire crews also face weather-aggravated dangers that often erupt quite suddenly due to the substantial *local* variability in weather conditions. Much of that variability occurs on our third critical time scale, ranging from *a few minutes to several hours* and over areas of perhaps 10-100 km square. It is on these short time scales, then, that front-line fire fighters may face some of their greatest threats because of the sudden, unexpected, localized nature of the changing environmental conditions. For example, a rapid reversal in the wind direction or an acceleration in speed can lead to shifts in the direction of a fire's advance, the transformation of smoldering embers into intense walls of heat and flame, or the rapid lofting and transport of hot embers across fire breaks. The localization of weather conditions is enhanced in regions of complex terrain, which can substantially distort the winds and can induce or reorganize the distribution of clouds and convective storms. Existing models run at NCEP lack the spatial and temporal resolution needed to provide this type of short-term, localized guidance. Thus, the U.S. Forest Service and other stakeholders could benefit from the development of more accurate and timely meteorological *nowcasts* for rapid response at these localize scales.

1.2 *Approaches for Short-Term Weather Products*

Based on the above scale analysis, two approaches present themselves for providing better short-term weather guidance to support forest-fire operations in the field. The first is to simply extend the present mesoscale-prediction scenario by adapting an existing numerical model to provide finer-resolution forecasts. High-resolution research models have been developed in recent years to produce real-time forecasts of 1-3 days into the future (e.g, Mass and Kuo 1998). Generally, these models are run *twice per day on fixed domains*. They can require fairly extensive computer resources, especially if the horizontal resolution is less than ~12 km. For very fine grids (Δx ~ 3-5 km), the area covered by such models is usually quite small. For a static domain large enough to cover an entire region of responsibility for the U.S. Forest Service (say, ~1200 km X 1600 km, or more), the use of a very fine grid is currently impractical without a rather expensive investment in the computer hardware. In addition, there are data-ingest and physics considerations that make it difficult to apply the standard existing models at ever-finer resolutions. Thus, given present computational limitations, regional numerical model designs with fixed-area domains are likely to be too expensive to operate routinely at resolutions having $\Delta x \leq$ ~10 km.

The second approach is to use *rapidly relocatable fine-mesh grids* to produce continuous nowcasts and very short-range forecasts (0-3 h). Using inexpensive computers with currently available processor speeds, new model updates can be supplied as frequently as every 30 minutes. The short time scale of these nowcasts is ideally suited for supporting fire crews in the field, where rapid updates of current conditions can be critical to the safety of personnel dispersed over remote, rugged areas. By using an intelligent design, a modeling system of this type can be made to run in real time, continuously assimilate new observations, and have very fine-grid domains that can be easily moved to cover areas currently experiencing fires. To build such a flexible and powerful modeling system, it is important to take advantage of several recent advancements in computing and atmospheric modeling:

(1) Rapid increases in processor speeds (now at 2 GHz) available in inexpensive PCs,
(2) Code optimizations developed for a mature mesoscale meteorological model widely used in the research and prediction communities,
(3) Advancements in physics parameterizations and practical data assimilation techniques, and
(4) Operational automation that allow users with little meteorological or numerical training to relocate domains and run a high-resolution model.

It is this type of flexible, easy-to-use advanced meteorological nowcasting and short-range forecasting system that is the subject of this demonstration study.

2. NOWCAST MODEL DESCRIPTION

To address the need for timely high-resolution meteorological guidance for a variety of applications, including forest-fire meteorology, a versatile nowcast numerical-modeling system has been developed at the Pennsylvania State University. Referred to as the *Relocatable Nowcast Mesoscale Model (RNMM),* the nowcast system is designed around a full-physics version of the non-hydrostatic Penn State/NCAR mesoscale model, MM5 (Grell et al. 1994). The MM5 is a nested-grid primitive equation model written in the terrain-following sigma vertical coordinate (non-dimensionalized pressure). For efficiency the MM5 uses a split semi-implicit temporal integration scheme. Triply nested grids of 36-, 12- and 4-km are used in the RNMM, each having 30 layers in the vertical direction. The model top is at 50 hPa The outermost domain covers an area of 3600 X 3600 km. The nested 12-km domain covers 1500 X 1500 km and the 4-km domain covers 500 X 500 km. For this demonstration, the domains are centered over the Cascade Mts. of Oregon (43 N, 122 W), where a large number of major fires were burning out of control in August of 2001. The locations of the two inner domains are shown in Figure 1, while the terrain on the 4-km domain is shown in Figure 2.

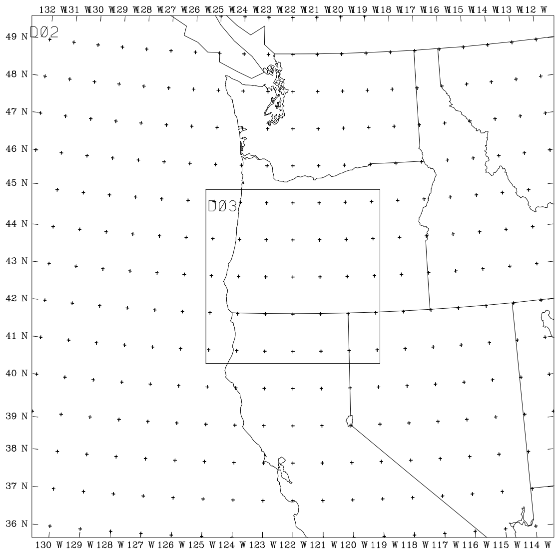

Figure 1. Location of the 12-km and 4-km domains of the demonstration version of the RNMM based on MM5.

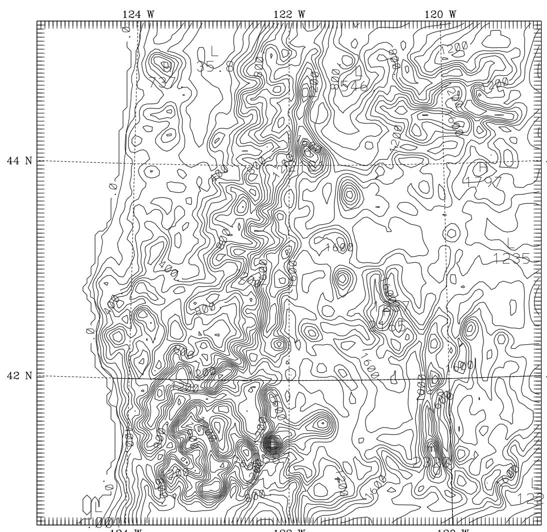

Figure 2. Terrain (m) for the 4-km innermost domain of the demonstration version of the RNMM based on MM5. Contour interval is 100 m.

The model physics for resolved-scale precipitation includes explicit prognostic equations for the mixing ratios of cloud water/ice (q_c) and rain/snow (q_r) (Dudhia 1989). Sub-grid deep convection is parameterized on the 36-km and 12-km domains using the scheme of Kain and Fritsch (1990). All precipitation processes are assumed to be resolvable on the 4-km domain (no parameterized convection necessary). The turbulence is represented in the RNMM using a 1.5-order closure scheme that explicitly predicts the turbulent kinetic energy (TKE) (Shafran et al. 2000, Stauffer et al. 1999). Long- and short-wave radiation contributions to temperature tendencies are calculated using a full-column broadband two-stream method (Duhdia 1989).

Figure 3 shows a schematic diagram indicating the main program functionality and the flow of data through the RNMM system. Processing of the initial conditions and boundary conditions (IC/BCs) is shown at the top of the figure and is based currently on real-time global-model fields supplied from the U.S. Navy's NOGAPS model. A "Conveyor Belt" module is used to store the incoming NOGAPS fields and select for processing those needed by the MM5 for the current time. The IC/BC Generator allows the RNMM to be initialized at any current wall clock time, rather than at specific traditional times (0000 and 1200 UTC). Meanwhile, a real-time data stream, such as Unidata, supplies the incoming observations (lower part of Figure 3). The GateKeeper module selects for processing only the newest observations that have arrived during the past 30 minutes. These new data are quality-checked in the Rawins-QC module by comparing the observations against the latest model solutions (interpolated to pressure levels by the Interp module) and through "buddy checks" against data from nearby sites. The RNMM system performs four-dimensional data assimilation (FDDA) to reduce numerical errors by blending new observations directly into the MM5 solutions as the model runs using the "observation-nudging" technique of Stauffer and Seaman (1994). The Prepobs/Chronobs module performs the final preparation of the quality-checked data for use in the MM5's FDDA system by projecting to the model's grids and collecting all observations processed during the previous 4 h (the maximum data "staleness" allowed in the RNMM). Processing of IC/BCs and the observations used in FDDA is done on a dual-processor 500 MHz PC.

For this application, the MM5 has been optimized for rapid execution on PCs using the Linux operating system. The RNMM runs in real time on an inexpensive dual-processor 933-MHz PC computer and produces new meteorological nowcasts of current conditions every 30 minutes. Each 30-minute nowcast segment requires a total of ~26 minutes of CPU for all three domains. Once a nowcast segment is completed the model automatically pauses to allow the wall clock to catch up before beginning the next 30-minute segment. The model domains can be relocated anywhere in the world in less than 5 minutes by an operator with minimal meteorological or numerical training.

The result is a continuous stream of highly detailed nowcasts that provide timely guidance about meteorological conditions as they develop over remote areas and complex terrain. Further work is expected to allow assimilation of new data types (such as satellite cloud-tracked winds) in real time, post-processing to reduce remaining errors in the model-generated products, and coupling to a plume-dispersion model for tracking airborne materials, such as smoke plumes.

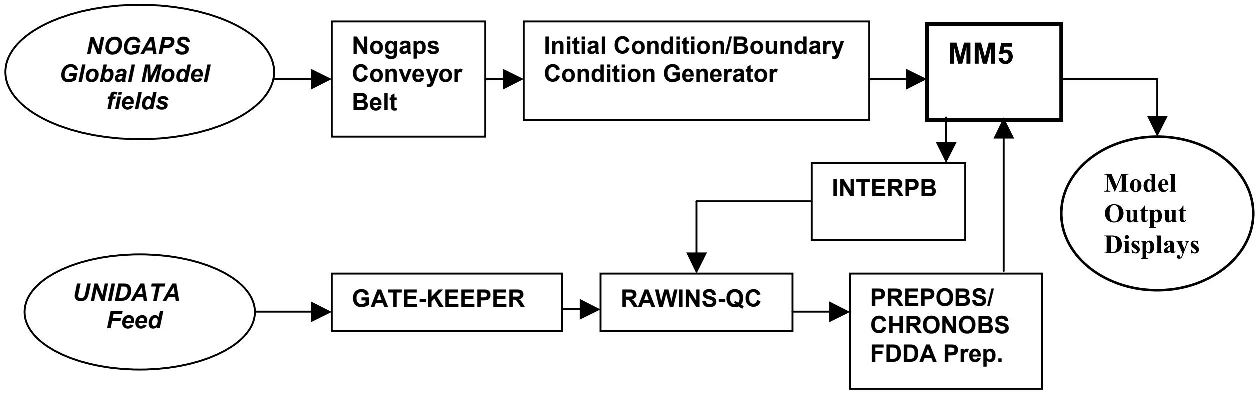

Figure 3. Schematic showing data flow through the RNMM system.

3. CASE DESCRIPTION AND METHODOLOGY

The case selected to demonstrate the RNMM is taken from 22-25 August 2001. This period is significant because it includes the passage of a cold front that brought rain and cooler temperatures to the Cascade Mts. and enabled fire crews to gradually bring under control many of the serious fires that had been burning out of control in OR and northern CA. Figure 4 presents a visible satellite picture from GOES-10 at 1830 UTC on 22 August, showing the cold front making landfall along the OR coast. Most of the precipitation fell on 22-23 August, with totals in OR reported to be 1.0 - 1.5 inches west of the Cascades and generally less than 0.15 inch to the east. Farther north in WA, rainfall in the western Cascades and Olympic Mountains ranged from about 2-8 inches. Figure 5 shows rainfall in the Pacific Northwest for the 24 h ending at 1200 UTC, 23 August, when most of the rain in OR was observed. By 24 August, skies had cleared over OR, CA and NV, and only isolated late-afternoon showers were reported over a few mountain peaks.

The model was initialized at 0200 UTC on 22 August and was operated continuously in real time for the next 70 h (final time was 0000 UTC, 25 August). Two experiments were run simultaneously on separate PCs. The first (Exp. FDDA) included FDDA for winds (surface and upper-air) and mass (temperature and mixing ratio above the boundary layer). The second (Exp. CNTL) did not use FDDA and was used as a control for comparison. Nowcasts were generated every 30 minutes during the exercise, with new BCs supplied every 12 h from the latest NOGAPS run. The BCs were the only source of new data influencing Exp. CNTL, while Exp. FDDA was also updated continuously through the assimilation of the current observations as the nowcast cycle proceeded.

Automated verification software was developed so that most statistical evaluation can be done on a daily basis as the model is integrated. Model errors are saved by the verification package for each hour, so that further in-depth evaluations can be done at a later time.

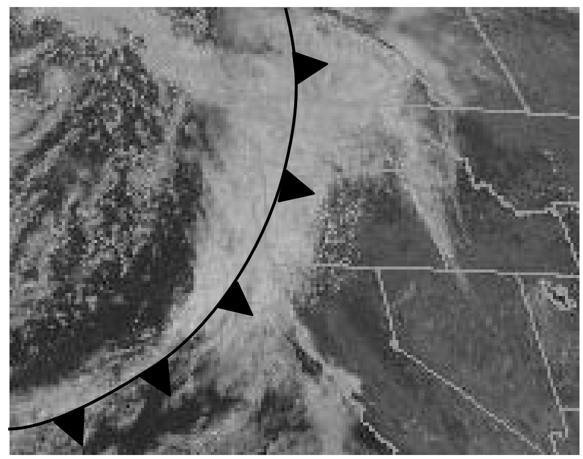

Figure 4. GOES-10 visible image for 1830 UTC, 22 August 2001. (Frontal position is from NCEP analysis.)

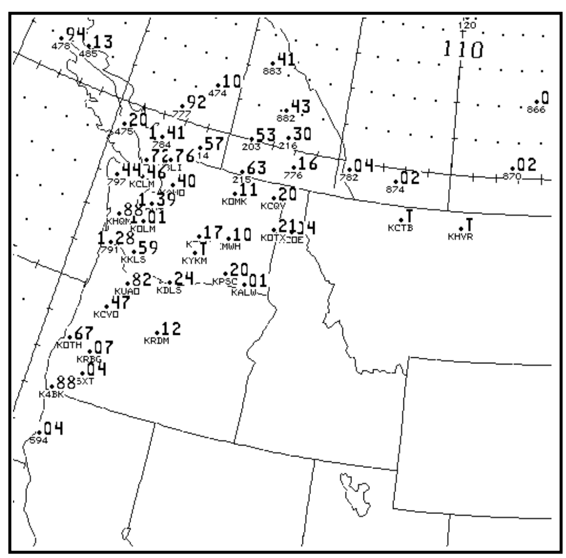

Figure 5. Observed precipitation totals over the Pacific Northwest for the 24-h period ending 1200 UTC, 23 August 2001.

4. RESULTS OF MODEL DEMONSTRATION

Visual comparisons of the individual fields generated by the two model experiments revealed generally similar patterns for most variables. Therefore, in this section examples of the model results will be presented only from Exp. FDDA, while statistical analysis will be used to demonstrate the difference between the solutions of the two experiments. The skill added through data assimilation can be an important characteristic of the nowcast solutions.

First, Figure 6 shows the nowcasted sea-level pressure and frontal position on the 12-km domain at 1800 UTC, 22 August, after the RNMM had been running for 16 h (32 individual nowcasts). The frontal position matches quite well with the observed position shown in Figure 4, even though there are no upper-air observations over the Pacific Ocean available for the RNMM's FDDA system. Next, Figure 7 shows the rain totals on the 12-km domain summed over all of the nowcast segments for the 6-h period ending at 0000 UTC, 23 August. This is the period of most intense rainfall over OR during the 24-h period included in the observed rain totals given in Figure 5. During this 6-h period, the model produced the heaviest rains (over 1 cm) along the OR coast and the western slopes of the Cascades from central OR to southern BC. This pattern matches well with the observed rain distribution and with the current frontal position. To the west over the Pacific Ocean, Figure 7 shows some weak bands of showers associated with a post-frontal trough. Following this 6-h period, rain diminished along the coast, but continued at a slower rate over the western Cascades for the next 12 h. After 1200 UTC, 23 August, only some light rainfall associated with the post-frontal trough was reported in OR (not shown).

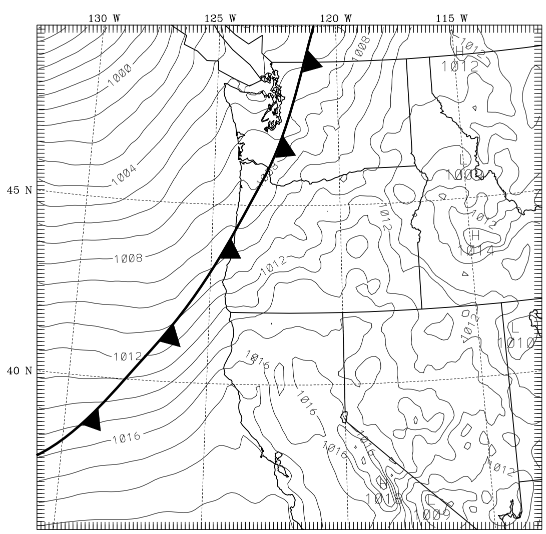

Figure 6. Sea-level pressure (HPa) simulated on the 12-km domain by the RNMM during the 30-minute nowcast segment ending at 1800 UTC, 22 August 2001. Isobars at 1 HPa intervals.

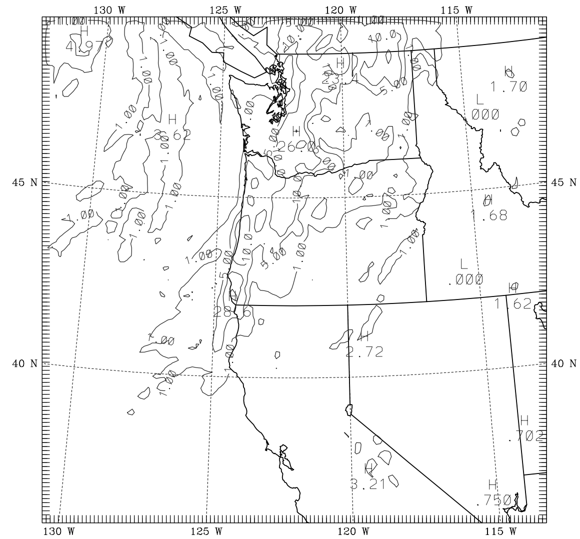

Figure 7. Total rainfall (mm) simulated on the 12-km domains by the RNMM summed over all 30-minute nowcast segments for the 6-h period ending at 0000 UTC, 23 August 2001. Contours shown for 1, 5, 10, 25 mm.

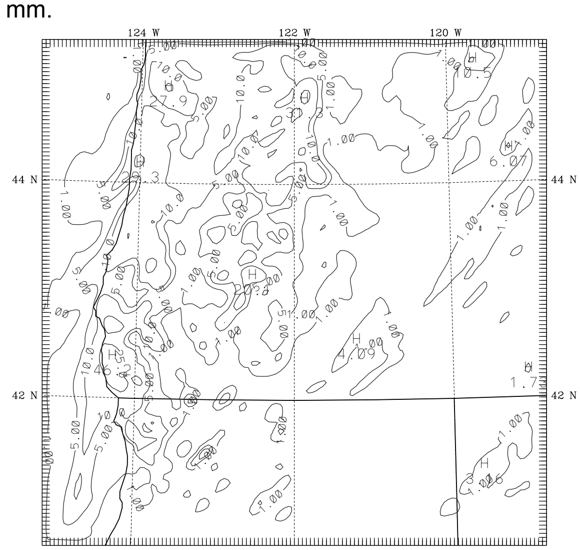

Figure 8. Same as Figure 7, except rainfall is shown on the 4-km domain of the RNMM.

Figure 8 shows the total rainfall on the 4-km domain summed over all nowcasts for the same 6-h period ending at 0000 UTC, 23 August (see Figure 7). The rainfall on the 4-km domain is mostly consistent with the 12-km rain for the same period, with totals greater than 1 cm along the OR coast and the western slopes of the Cascades. Isolated pockets of 2.5 cm rain (~1 inch) are also evident near some of the highest peaks. Notice that the precipitation east of the Cascades is very light (~1-4 mm) and appears mostly in bands aligned from southwest to northeast, along the mean lower-tropospheric wind direction in the pre-frontal zone. This elongation of the rain "footprints" is typical of isolated convective showers that last perhaps

0.5-2.0 h or so. In contrast, the rain west of the Cascade divide is broadly distributed and oriented with the mountains. This pattern is typical of the non-convective (stable) upslope rainfall mechanism. Thus the 4-km model solution suggests that lightning associated with the convection on the east side of the Cascade Range could easily ignite fires about this time. In fact, when a model produces only 1-2 mm of rain in such a dry environment, there is considerable uncertainty about whether any rain will actually be measured at the surface.

In addition to information about the rainfall type and distribution, winds are one of the most important variables for which short-term nowcasts are desirable. Figure 9 shows the surface-layer winds simulated by the RNMM at 40 m above ground level (AGL) for 1800 UTC, 22 August. The figure, which also shows current observations superimposed, indicates moderately strong winds just west of the coast (10-15 ms^{-1}) with light to moderate winds over OR (2-10 ms^{-1}). Most of the higher wind speeds over land occur on the windward side of the higher terrain because a southwesterly low-level jet existed just ahead of the frontal band as it approached land (not shown). In the lee of some of the highest peaks (e.g., the Three Sisters near 44.1 N, 121.8 W; see Figure 2), the surface winds become weak and variable, or may actually reverse direction.

The verifying winds in the figure indicate that the directions were simulated rather well by the model over most of the region, with only a few sizeable directional errors, mostly in the lee of major very-fine scale terrain. The surface wind speeds tend to average 1-2 ms^{-1} too fast, in part because the model simulates winds at 40 m AGL (the lowest layer is 80 m deep), while the standard height for the observations is 10 m. In addition, unresolvable small-scale terrain tends to be important in mountainous regions, contributing both to surface drag and directional variability. The unresolved drag can be accounted for quite easily in future applications and the effect of the 80-m surface layer can be addressed by simple post-processing or a thinner surface layer.

Finally, Tables 1 and 2 summarize performance of the RNMM in the two demonstration experiments using statistical scores. Three types of statistics are shown for wind speed and direction (Table 1) and for temperature, relative humidity and sea-level pressure (Table 2). First, the mean absolute error (MAE) gives the magnitude of the most typical model error for a given variable, which is usually a bit smaller than the root mean square error (not shown). The mean error (ME) gives the model bias for the variable. (The formulae for these quantities are reported by Stauffer et al. 1991). Lastly, for each variable, the percentage of model nowcasts verifying within an arbitrary threshold is presented. The threshold values (given in the table headings) are chosen arbitrarily, but are meant to represent a fairly strict measure of accuracy (except for pressure, with is less critical for the given application).

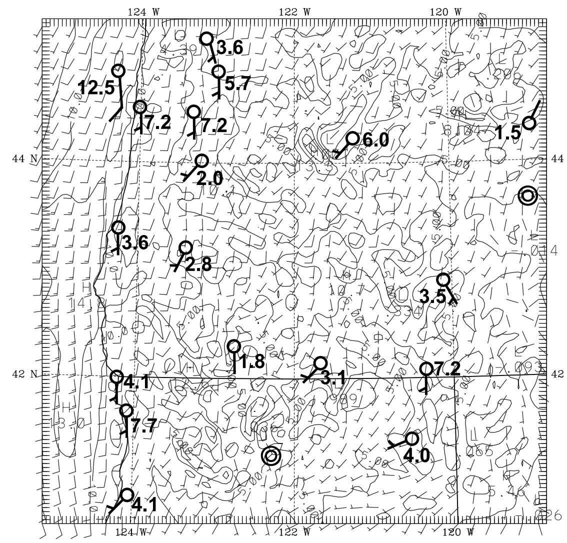

Figure 9. Surface-layer winds (ms^{-1}) simulated on the 4-km domain by the RNMM at 40 m AGL during the 30-minute nowcast segment ending at 1800 UTC, 22 August 2001. Isotach interval is 2.5 ms^{-1}.

In Table 1, it can be seen that Exp. FDDA significantly outperforms Exp. CNTL, indicating that the blending of observations into the model solutions in the real-time nowcasts has a very positive effect for reducing errors. The benefit is apparent at the surface, in the lowest kilometer (nominally, the approximate depth of the planetary boundary layer, or PBL), and the lower troposphere (1000 - 5000 m AGL). Note that the verification is performed at all observation sites inside the two respective domains (12-km and 4-km). Thus, the statistics cannot be compared exactly between the two domains in this case, because of the larger area of the 12-km domain. Nevertheless, the statistical skill for the winds is very similar to that reported for numerical simulations (with FDDA) of episodes having poor air-quality reviewed by Seaman (2000). This is quite encouraging, since the air-pollution cases were run on historical cases having abundant special observations and the data could be assimilated both before and after the actual observation times. In the real-time nowcasts, no special data were available and the data could only be used after they arrived over the Unidata circuit.

Likewise, Table 2 shows significant reduction in model errors for Exp. FDDA, relative for Exp. CNTL, in the layers *above* the surface (no surface temperatures are assimilated in the current methodology). There is little no impact found due to the FDDA in the sea-level pressure. Pressures are not assimilated directly, although adjustment of the winds and temperatures can affect the pressures, at least indirectly. For the purpose of forest-fire meteorology, it is especially encouraging that there is relatively small bias (ME) and variance (MAE) in the relative humidities. This indicates rather good indication of moist versus dry air in the nowcasts. As found for the winds, the statistics for these mass field variables are comparable to those reported by

Seaman (2000) in air-pollution cases with special data and the benefit of pre-observation-time FDDA.

5. SUMMARY AND FUTURE DIRECTIONS

A real-time relocatable nowcast system has been constructed and demonstrated to have potential benefits for assisting fire fighters to anticipate and respond to short-term meteorological variability at very fine (4-km) resolution. With modest effort, the current demonstration system can be improved in the areas of data ingest, sub-grid physics, the FDDA approach, and post-processing. The data can be augmented by adding satellite cloud-tracked and vapor-tracked winds, ACARS winds, etc. Physics of the land surface can be improved by accounting for time-varying soil moisture. The FDDA approach can be improved by developing strategies for assimilating mass field data in the PBL. Post-processing of the nowcasts would help reduce the remaining bias errors and would correct for the mismatch in height between the model's surface layer and the surface-observation level. Moreover, the current 30-minute nowcast can be augmented with short-range forecasts of 0-3 h.

6. ACKNOWLDGEMENTS

Support for this study was provided by ETG, Inc., under contract from the U.S. Army, through Contract No. PPQ001. Carlie Coats of MCNC provided valuable assistance to optimize portions of the MM5 code.

Table 1. Verification of nowcasted winds simulated by the RNMM for 70 h during the case of 22-25 Aug. 2001 versus all observations in each domain. Statistics shown in parentheses are for the initial surface conditions interpolated from NOGAPS fields. Right-hand column indicates percentage of model winds that are accurate within a speed threshold of 2.5 m/s and a direction threshold of 12 degrees.

Variable	Layer/Exp.	Mean Abs. Errors (m/s)			Mean Errors (m/s)			% Verifying Within Threshold		
Wind Spd. (m/s)		NGP Ics	12 km	4 km	NGP Ics	12 km	4 km	NGP Ics	12 km	4 km
								[Wind Spd Threshold = 2.5 m/s]		
	Sfc. Layer **<u>40 m AGL</u>**	(2.80)			(-1.45)			(50.0%)		
	Exp. CNTL		2.11	2.23		+0.63	+1.18		65.7%	63.2%
	Exp. FDDA		1.67	1.66		+0.20	+0.50		77.2%	77.6%
	PBL **<u>80-1000 m</u>**									
	Exp. CNTL		3.56	6.77		+1.77	+4.12		49.6%	5.5%
	Exp. FDDA		2.49	3.68		+0.60	+2.22		65.0%	25.0%
	Low Trop. **<u>1000-5000m</u>**									
	Exp. CNTL		2.92	4.67		+0.73	+1.10		47.1%	18.5%
	Exp. FDDA		1.94	2.65		+0.35	+1.39		72.2%	48.1%
Wind Dir. (deg)		NGP Ics	12 km	4 km	NGP Ics	12 km	4 km	NGP Ics	12 km	4 km
								[Wind Dir Threshold = 12 deg.]		
	Sfc. Layer **<u>40 m AGL</u>**	(55.5)			(15.8)			(12.4%)		
	Exp. CNTL		49.0	48.2		+10.8	+ 4.6		19.9%	22.3%
	Exp. FDDA		38.3	35.7		+ 7.8	+ 1.9		26.7%	28.1%
	PBL **<u>80-1000 m</u>**									
	Exp. CNTL		51.7	32.7		+18.8	+24.6		27.1%	47.2%
	Exp. FDDA		45.0	30.2		+10.9	+12.1		37.4%	55.5%
	Low Trop. **<u>1000-5000m</u>**									
	Exp. CNTL		29.4	11.3		+15.3	+ 2.5		33.9%	59.2%
	Exp. FDDA		18.3	7.9		+14.2	+ 0.9		50.4%	72.2%

7. REFERENCES

Barnston, A.G., A. Leetmaa, V.E. Kousky, R.E. Livezey, E. A. O'Lenic, H. Van den Dool, A.J. Wagner, and D.A. Unger, 1999: NCEP forecasts of the El Nino of 1997-98 and its U.S. impacts. *Bull. Amer. Meteor. Soc.*, **80**, 1829-1852.

Black, T.L., 1994: NMC Notes: The new NMC Mesoscale Eta Model: Description and forecast experiments. *Wea. and Forecasting*, **2**, 266-278.

Dudhia, J., 1989: Numerical study of convection observed during the Winter Monsoon Experiment using a mesoscale two-dimensional model. *J. Atmos. Sci.*, **46**, 3077-3107.

Table 2. Verification of nowcasted temperature, relative humidity, and sea-level pressure simulated by the RNMM for 70 h during the case of 22-25 Aug. 2001 versus all observations in each domain. Statistics shown in parentheses are for the initial surface conditions interpolated from NOGAPS fields. Right-hand column indicates percentage of model temperatures that are accurate within a threshold of 2.0 C, humidities within a threshold of 10 % and pressures within a threshold of 3.0 mb. Asterisks in "Layer/Exp" column indicate variables/levels where FDDA is not applied.

Variable	Layer/Exp.	Mean Abs. Errors (C)			Mean Errors (C)			% Verifying Within Threshold		
Temp. (C)		NGP Ics	12 km	4 km	NGP Ics	12 km	4 km	NGP Ics	12 km	4 km
								[Temp. Threshold = 2.0 C]		
	Sfc. Layer **<u>40 m AGL</u>**	(3.31)			(-2.17)			(33.9%)		
	Exp. CNTL		2.83	2.24		-1.83	-0.98		45.1%	53.4%
	*Exp. FDDA		2.80	2.23		-1.79	-0.95		46.5%	53.2%
	PBL **<u>80-1000 m</u>**									
	Exp. CNTL		3.41	1.11		-3.03	-1.02		37.9%	72.2%
	*Exp. FDDA		2.94	0.93		-2.71	-0.92		48.6%	83.3%
	Low Trop. **<u>1000-5000m</u>**									
	Exp. CNTL		2.22	0.64		-2.04	-0.27		50.4%	94.4%
	Exp. FDDA		1.84	0.50		-1.82	-0.36		66.1%	100.0%
Rel. Hum. (%)		NGP Ics	12 km	4 km	NGP Ics	12 km	4 km	NGP Ics	12 km	4 km
								[Rel. Hum. Threshold = 10%]		
	Sfc. Layer **<u>40 m AGL</u>**	(14.0)			(-0.8)			(38.5%)		
	Exp. CNTL		12.9	12.0		+ 5.3	+ 3.6		47.5%	50.5%
	*Exp. FDDA		12.7	12.1		+ 4.6	+ 2.8		48.3%	49.73%
	PBL **<u>80-1000 m</u>**									
	Exp. CNTL		15.3	7.9		+10.4	+ 2.2		47.3%	77.8%
	*Exp. FDDA		11.5	4.9		+ 9.2	+ 2.5		55.3%	91.7%
	Low Trop. **<u>1000-5000m</u>**									
	Exp. CNTL		15.7	13.8		+ 9.6	+ 7.5		43.8%	57.4%
	Exp. FDDA		11.1	8.2		+ 8.3	+ 3.6		58.3%	81.5%
S.L. Pres. (mb)		NGP Ics	12 km	4 km	NGP Ics	12 km	4 km	NGP Ics	12 km	4 km
								[S.L. Pres. Threshold = 3 mb]		
	<u>Sea Level</u>	(1.67)			(-0.41)			(87.8%)		
	Exp. CNTL		1.78	1.20		+0.19	+0.00		84.5%	97.3%
	*Exp. FDDA		1.81	1.25		-0.04	-0.12		83.6%	97.2%

Grell, G.A., J. Dudhia and D.R. Stauffer, 1994: A description of the fifth-generation Penn State/NCAR Mesoscale Model (MM5). NCAR Technical Note NCAR/TN-398+STR, 121 pp.

Jackson, R., 2001: Tragedy re-ignites wildfire debate. *High Country News*, **33**, Issue 14, 30 July, http://www.hcn.org/servlets/hcn.Article?article_id=10626

Mass, C.F. and Y.-H. Kuo, 1998: Regional real-time numerical weather prediction: Current status and future potential. *Bull. Amer. Meteor. Soc.*, **79**, 253-263.

Seaman, N.L., 2000: Meteorological modeling for air-quality assessments. *Atmos. Environ.*, **34**, 2231-2259.

Shafran, P.C., N.L. Seaman and G.A. Gayno, 2000: Evaluation of numerical predictions of boundary layer strucutre during the Lake Michigan Ozone Study. *J. Appl. Meteor.*, **39**, 412-426.

Stauffer, D.R., R.C. Munoz and N.L. Seaman, 1999: In-cloud turbulence and explicit microphysics in the MM5. Preprints, 9th PSU/NCAR MM5 Modeling System User's Workshop. Boulder, CO, 23-24 June, 177-180.

Stauffer, D.R., and N.L. Seaman, 1994: Multiscale four-dimensional data assimilation. *J. Appl. Meteor.*, **33**, 416-434.

Stauffer, D.R., N.L. Seaman and F.S. Binkowski, 1991: Use of four-dimensional data assimiltion in a limited-area mesoscale model, Part II: Effects of data assimilation within the planetary boundary layer. *Mon. Wea. Rev.*, **119**, 734-754.